Author/s:
Liu, L;Lee, JH;Han, SH;Ha, SY;Chen, GQ;Kentish, SE;Yeo, JG

Title:
Assessment of Membrane Performance for Post-Combustion CO2 Capture

Date:
2022-01-12

Citation:
Liu, L., Lee, J. H., Han, S. H., Ha, S. Y., Chen, G. Q., Kentish, S. E. & Yeo, J. G. (2022). Assessment of Membrane Performance for Post-Combustion CO2 Capture. Industrial and Engineering Chemistry Research, 61 (1), pp.777-785. https://doi.org/10.1021/acs.iecr.1c03987.

Assessment of membrane performance for post combustion CO_2 capture

Liang Liu[1,2†], Jung Hyun Lee[3,†], Sang Hoon Han[4], Seong Yong Ha[4], George Q. Chen[1], Sandra E. Kentish[1,], Jeong-gu Yeo[3,*]*

1 Department of Chemical Engineering, the University of Melbourne, Vic. 3010, Australia

2 CSIRO Mineral Resources, 1 Technology Court, Pullenvale, Queensland 4069, Australia

3 Energy Conversion & Storage Materials Laboratory, Korea Institute of Energy Research, Daejeon, 34129, Korea

4 Airrane Co. Ltd., Cheongju, 28121, Korea

[†]First author

*Corresponding author.

E-mail address: sandraek@unimelb.edu.au, jgyeo@kier.re.kr

Abstract

This work investigates the separation performance of a commercial carbonised polyimide hollow fibre membrane module for post-combustion CO_2 capture applications. In particular, the resilience to water, sulfur and nitrogen oxides (SOx and NOx) as gas impurities was examined. The membrane exhibited a CO_2 permeance of 660 Gas Processing Units (GPU) and CO_2/N_2 permselectivity of 20 at 50 °C when the permeate side was controlled at 0.2 bar absolute pressure. With an increase in water vapor in the feed stream, this CO_2 permeance dropped slightly while the CO_2/N_2 selectivity increased slightly, due to the combination of competitive sorption and concentration polarisation. The water vapor permeance was high, which made accurate measurement difficult due to the concentration polarisation but a value of 1090±200 GPU was recorded. The membrane was then examined under three mixed gas conditions (i.e $SO_2/CO_2/O_2/N_2$, $NO/CO_2/N_2$ and $NO/NO_2/N_2$) for a time frame of 30 days. The permeances of SO_2, O_2, NO and NO_2 were 650±50, 155±5, 125±10 and 70±5 GPU at 30 °C, respectively. All of these minor components had little impact on the membrane separation performance during the testing period, indicating strong commercial potential. The higher permeance of SO_2 and NO relative to nitrogen meant that these penetrants were concentrated in the permeate stream, which might lead to issues with downstream corrosion in a humid environment. Conversely, the permeance of NO_2 was low.

1. Introduction

The global warming issue attracts much attention in our society [1] and CO_2 emissions from fossil fuels are one of the most important contributors [2-4]. To limit the global temperature rise to below 2 °C, 95% of coal-fired power plants would need to implement CO_2 capture facilities [5] . Post-combustion CO_2 capture is very attractive as it can be easily integrated with existing coal-fired power stations. Solvent-based CO_2 capture is commercially available and can be integrated with porous non-selective membrane contactors to reduce capital cost[6-8]. However the use of non-porous CO_2-selective gas separation membranes can also be a competitor due to their high energy efficiency [9] and the avoidance of chemicals which can add complexity and environmental hazards to a power station.

Glassy polymeric materials are considered as potential candidates for use as such CO_2-selective membranes as they show good gas separation performance due to their rigid chain structure [10] and good processability. Among them, polyimide-based materials are promising because they exhibit both a higher selectivity and permeability than other polymer materials [11-14]. The most studies about membrane materials on CO_2 capture from post-combustion flue gas are basically focused on higher selectivity and permeability. Alongside CO_2 and N_2, flue gases from coal-fired power stations are also saturated with water and contain minor components such as SO_x and NO_x[15]. Although there are many reports of membrane performance for 'clean' CO_2/N_2 separation either as pure gases or combined, there are very few publications investigating the impact of minor components (e.g. H_2O, SO_x and NO_x) on the membrane separation performance. However, the effect of minor component in post-combustion flue gas is not negligible in the design and operation of membrane process for carbon capture due to competitive sorption, plasticization and aging

effects on the membrane. [15] As such, it is necessary to address these technical and operational concerns before commercialization of the membrane capture process.

Water vapor can have different impacts on the separation performance depending on the membrane composition. The vapor molecules can compete with other gases for sorption sites in a glassy polymer, thus reducing its permeability. Ansaloni et al. reported that CO_2, N_2 and CH_4 permeabilities in Matrimid 5218 decreased when water vapor content in the membrane increased [16]. Similarly, Scholes et al.[17] observe a loss of both CO_2 and CH_4 permeability, but no change in selectivity when a thermally re-arranged (TR) polyimide was exposed to water vapor. Conversely, water vapor can swell or plasticize a hydrophilic membrane at high water concentration, resulting in an increase of gas permeability and decline of selectivity [18]. Anderson et al.[19] observed no change in performance for a nanoporous carbon membrane upon the addition of up to 0.25 mol% water vapor, reflecting the resistance of such structures to plasticisation. However, water permeance is generally higher than that of the other gases, so can be rapidly depleted from the feed stream in a commercial scale module [20]. Further, if the water permeance is significantly higher than the other gases, concentration polarisation effects can be significant. As a result, the influence of water vapor on the performance of a new membrane material requires thorough investigation.

Flue gases from coal fired power stations typically contain 200–5000 ppm SOx, but flue gas desuphurization can reduce this to between 10 and 50ppm[21]. Many polymeric membrane materials are SO_2 selective because of its high condensability [4, 22, 23]. Permeabilities, diffusivities as well as activation energy for the permeation of SO_2 has been recorded for various polymers [23]. Recently, it has been reported that a Pebax/PEI hollow fiber membrane exhibited a SO_2 permeance of above 1500 GPU (1 GPU = 10^{-6} cm^3_{STP}/cm^2.s.cm Hg) and SO_2/CO_2 selectivity over 60 at 30 °C [22]. Lu et al. [4] reported a SO_2 permeability of 20 barrer (1 barrer = 10^{-10} $cm^3_{STP}.cm/cm^2$.s.cm Hg) for a

thick CTA membrane under 1000 ppm SO_2 feed condition at 35 °C and SO_2/N_2 selectivity over 100.

SO_2 is more condensable than CO_2 and so can plasticize the polymer, but it can also compete with CO_2 for sorption sites, leading to a reduction in CO_2 permeability. In tests with a polycarbonate membrane, a short-term test did not reveal any significant impact on CO_2 permeability, but 20% loss of permeance was shown after continuous exposure to 300 ppm SO_2 over a 4-month period [24]. Wang et al. investigated the effect of SO_2 on a facilitated transport membrane using a mixed feed gas containing 5000 ppm of SO_2 and showed that the CO_2 permeance declined by 17% and the CO_2/N_2 selectivity by 20% due to the competitive sorption. [25]

Nitric oxide in flue gases ranges from 10 to 500 ppm, mostly as NO and traces as NO_2 [15]. Scholes et al. found that NO had a permeance greater than N_2 but less than that of CO_2 for glassy polymers such as polysulfone, Matrimid 5218 and 6FDA-TMPDA [26]. Recently, Lu et al. [4] reported that the NO concentration on the permeate side was under the detection limit for a 3 μm CTA membrane, suggesting the NO permeability was below 4 Barrer at 35 °C. More importantly, however, they showed that the aging rate was much faster for the CTA membrane exposed to NO_x and it was suggested that trace amounts of NO_2 could oxidize the primary alcohol of cellulosic materials, resulting in a decline of gas permeability. It is clear that such information is important to evaluate the membrane performance. There is very little data on the effect of NO_2 in these systems, but Pasternak et al.[27] observed that while NO_2 has approximately the same size as CO_2, its diffusion coefficient in a PTFE membrane was smaller. Conversely, its solubility in PTFE was much larger due to its polar nature interacting strongly with the PTFE, which led to a NO_2/CO_2 selectivity of around 13.

It is well-known that aging can occur in glassy polymers and the rate depends upon the material properties, thickness and operating conditions [28, 29]. There have been some studies that report significant performance changes arising from this effect. For instant, 6FDA-DAM thin films of 300-1000 nm showed an order of magnitude decrease in permeability over the course of 1000 h of aging. On the other hand, a thick 6FDA-DAM film of 41 μm maintained its permeability over 1000 h of aging [28]. There are other studies that report membrane durability with flue gases containing a mixture of water vapor, SO_x and NO_x components. The PolyActiveTM membrane was tested for 740 hours at pilot scale using a real flue gas from a power plant, which contained 14.5% CO_2, 6.5% O_2, 50-100 ppm of SO_2 and 76-91 ppm of NO_x and 14% of H_2O by Brinkmann et al. [4]. In another study, a hollow fiber module made from a polyvinyl amine (PVAm) based facilitated transport membrane was tested for 24 days with a cement factory flue gas containing 15-19% of CO_2, 100 ppm of SO_2 and 5 ppm of NO_x, respectively[30]. The membrane provided good stability without significant performance change.

This work studies the CO_2/N_2 separation performance of a carbonised polyimide hollow fibre membrane formed through phase inversion for post-combustion CO_2 capture application. First, the membrane is examined using dry CO_2 and N_2. Then the influence of water vapor on the performance of the membrane is investigated. Finally, the membranes are tested for three different gas mixtures including an $SO_2/CO_2/O_2/N_2$ mixture, $NO/CO_2/N_2$ mixture and $NO/NO_2/N_2$ mixture over the course of 30 days. We believe that this is the first report of the impact of such impurities on the performance of a carbonised membrane, particularly over such extended timeframes.

2. Experimental

2.1. Humid Gas Testing

The membrane module of 895 cm^2 surface area was provided by Airrane Co. Ltd. It was comprised of carbon molecular sieve hollow fibres prepared by carbonizing a polyimide precursor, as described in detail in previous work [31, 32] A hollow fibre membrane module was tested for N_2 and CO_2 permeance as single gases and in mixtures with water vapor at 50 °C using the apparatus shown in Figure 1[33]. The membrane module was kept in a convection oven at a constant temperature during the test.

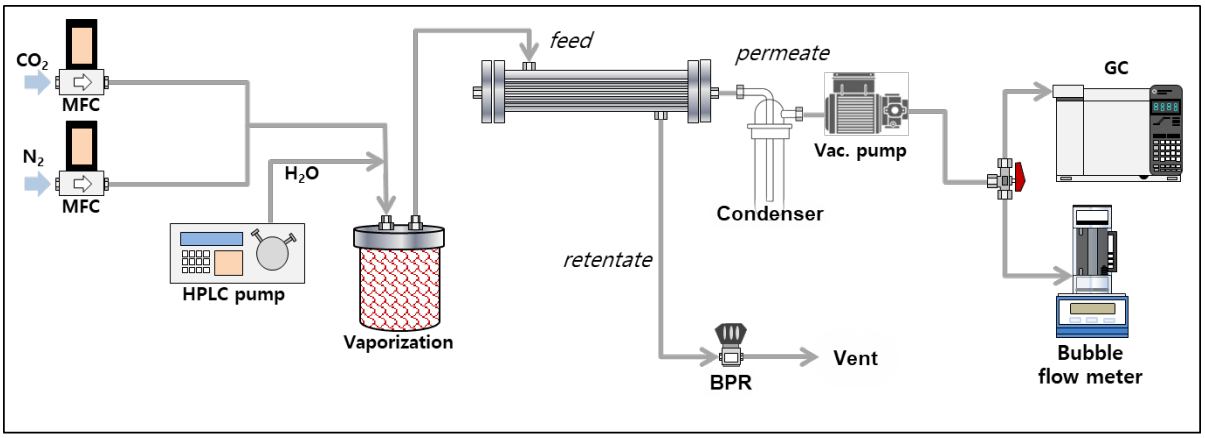

Figure 1. Schematic of the humid gas permeation rig.

The flow rate of each gas component and the mixed gas composition at the feed side was individually controlled using a mass flow controller (MFC). Single gases (CO_2 or N_2) and a mixture of 14/86 (v/v, CO_2/N_2) were purchased from the Special Gas Company in Korea. The feed gas flow rate was set to 0.22 Nm^3/h for single gas tests and 0.5 Nm^3/h for mixed gas tests. Mass flow controllers (5850E, Brooks Inst. Ltd., USA) were calibrated for each gas component with a

conversion factor that was obtained from the ratio of the setting value to the real gas flow rate, which was measured using a bubble flowmeter (Gilibrator 2, Sensidyne, FL, USA). The compositions of the gas mixtures were confirmed by gas chromatography (GC, Agilent 7890B, Santa Clara, CA, USA). A series of packed columns (10 ft × 1/8-inch Porapak N and 3 ft × 1/8-inch Molesieve 13X) and an on-line thermal conductivity detector (TCD) was used for GC analysis. A calibration curve was generated from 5% to 95% CO_2 at N_2 balance.

For the experiments under humid conditions, water vapor was added to a gaseous mixture (CO_2 and/or N_2) using a digital plunger pump (NP-KX 200, Nihon Seimitsu Kagaku Co., Ltd., Japan). The absolute amount of added water was calculated from the vapor pressure of water at a given temperature. The vaporization step was conducted at temperatures over 230 °C so that the water vapor was totally evaporated and mixed with the gaseous mixture to create humid gas mixtures. The temperature, humidity and pressure of this gas mixture was confirmed by a multifunctional transmitter (EE31, Elektronik, Austria) and pressure transmitter (EJA 530E, Yokogawa, Japan), respectively. The whole membrane system as well as the heating and mixing unit were kept at a given temperature and pressure to prevent water vapor condensation.

The feed stream was directed to the shell side of the hollow fiber module, where the permeate stream was collected from the bore side of the module, with flow counter-current to the feed direction. The feed pressure was regulated by a back-pressure regulator on the retentate side at either 1.2 or 2.0 bar. For experiments with a feed pressure of 1.2 bar, the pressure of the permeate side was controlled at 0.2 bar by a vacuum pump (DTC-21, Ulvac, Inc., Japan). For experiments with a feed pressure of 2 bar, the permeate flow rate was recorded at either ambient pressure (1 bar) or 0.3 bar.

On the permeate side, the relative humidity of the permeate gas was detected using a multifunctional transmitter immediately after the membrane. The relative humidity was converted to a water partial pressure (p_i,bar) using the Antoine equation to determine the saturation partial pressure(p_i^*,bar) at the measurement temperature (T, in ºC) (Equation 1).

$$Relative\ humidity = \frac{p_i}{p_i^*} = \frac{p_i}{0.001333x10^{8.071-\frac{1731}{233.4+T}}} \quad (1)$$

Before measurement of the CO_2/N_2 composition and the flow rate of the gas mixture at the permeate side, permeated water vapor was condensed by a low temperature trap.

2.2. Minor Component Testing

The influence of three minor gases (i.e. SO_2, NO and NO_2) on the membrane stability were tested in a custom built gas permeation rig shown in Figure 2. Briefly, the hollow fibre membrane module with a membrane surface area of 200 cm^2 was mounted in an oven with controlled temperature of 30 °C. The feed gas pressure was set at 2 bar by a pressure regulator and the retentate flow rate was set to 1.25 L/min by a mass flow controller. The permeate pressure was controlled at 0.2 bar by using a vacuum pump and a needle valve.

A Frontier FTIR Spectrometer (Perkin Elmer, USA) equipped with a CycloneTM gas cell was used to analyze the concentration of SO_2, NO or NO_2 during the membrane permeation test. The FTIR was calibrated against SO_2, NO or NO_2 across a range of pressures (0.1-1.1 bar) to generate the calibration curves. Prior to each experiment, a background scan was conducted under vacuum conditions. A 490 Micro GC (Agilent Technologies, USA) with a Micro-machined Thermal Conductivity Detector (μTCD) and a 10 m PoraPlot U (PPU) column was used to analyze permeate gas composition (i.e. N_2, O_2 and CO_2). The system was stabilized for at least 2 hours before

measurement. Each measurement was repeated 3-5 times. Each membrane module was tested periodically in this manner over a time frame of 30 days. During the periods between each experiment, the module was maintained at the feed gas conditions i.e. exposed to the relevant gas mixture at 2 bar on both the feed and permeate sides. All experiments were carried out in a walk-in fume booth to minimize safety concerns.

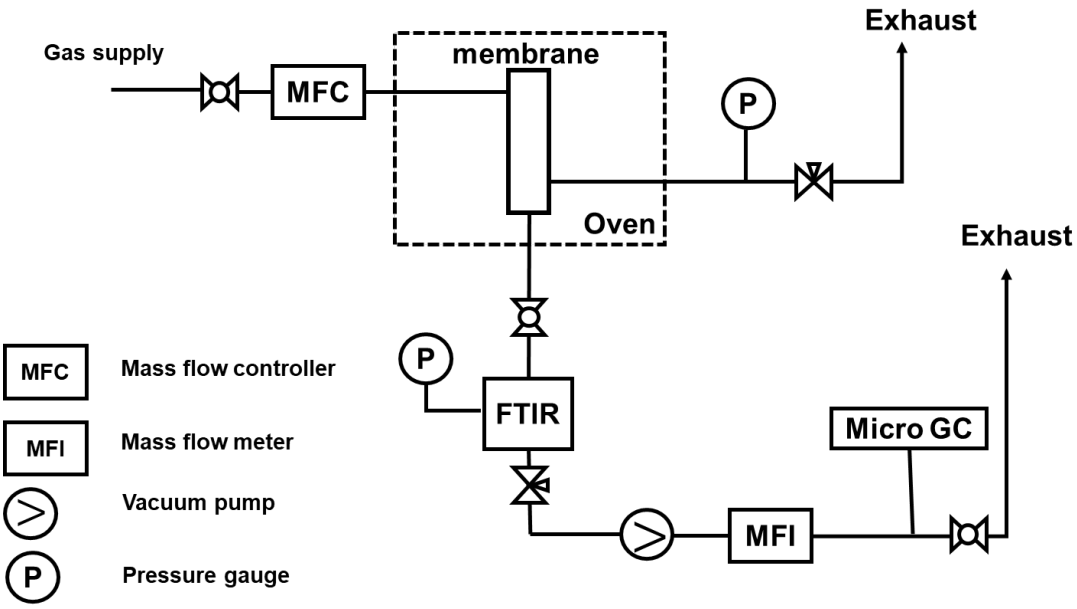

Figure 2. Schematic of the toxic gas permeation rig.

All three gas mixtures were Certified Calibration Standard and were supplied by BOC, Australia with the specific compositions as listed in Table 1. These concentrations were selected as they are typical of those likely to be present in a coal fired power station flue gas.

Table 1: Gas compositions used in the long term mixed gas experiments

	SO_2 (ppm)	NO (ppm)	NO_2 (vol%)	O_2 (vol%)	CO_2 (vol%)	N_2
Test 1	990			6.04	14	Balance
Test 2		990			13.4	Balance
Test 3		750	205			Balance

2.3. Data Analysis

In all cases, the gas or water vapor permeance was calculated from Equation 2:

$$P_i = \frac{J_i}{(p_{i,f} - p_{i,p})} = \frac{Q_t \cdot y_i}{A(p_{t,f} \cdot x_i - p_{t,p} \cdot y_i)} \quad (2)$$

Where P_i is the permeance of penetrant *i*; J_i is the transmembrane flux of gas *i* (cm^3(STP)/cm^2. min); $p_{i,f}$ and $p_{i,p}$ are the partial pressure of penetrant *i* in the feed and permeate side, respectively; $p_{t,f}$ and $p_{t,p}$ are the total pressure in the feed and permeate side (i.e. 2 and 0.2 bar).; A is the effective membrane area; Q_t is the total flow rate of the permeate stream (cm^3(STP)/min); $x_i$and y_i are the mol fraction of species *i* in the feed and permeate side determined by the relative humidity, the Micro GC or FTIR.

The CO_2 recovery was calculated from Equation 3:

$$Recovery = \frac{Q_t \cdot y_i}{F_t \cdot x_i} \quad (3)$$

Where F_t is the total flow rate of the feed stream (cm^3(STP)/min)

3. Results and Discussion

3.1. Humid Gas Testing

Figure 3 shows the influence of water vapor on the permeances of pure CO_2 and N_2 gas streams tested individually under three different total pressure conditions (i.e. 1.2/0.2, 2.0/1.0 or 2.0/0.3 bar, respectively). For dry N_2 the permeance was 36 ± 3 GPU across the three different pressure conditions. For dry CO_2 the permeance was 660 GPU respectively, when the feed pressure was 1.2 bar, but this increased to 739 ± 14 GPU when the feed pressure was 2.0 bar. The slight differences may indicate CO_2 plasticization at the higher feed pressures. With an increase in the water vapor partial pressure, the CO_2 permeance decreased slightly for all cases. The N_2 permeance also fell to 21 ± 1 GPU, so that the CO_2/N_2 selectivity increased slightly from 20 ± 1 to 28 ± 3. The decrease in CO_2 and N_2 permeance can be attributed to competitive sorption, as water has a much higher critical temperature than CO_2 and N_2 and also possibly to the formation of water clusters reducing the diffusivity of other gases [34]. To counterbalance this, as the water content increases, concentration polarisation will favor the permeation of the slower gases, leading to an apparently higher permeance than the true value. This tradeoff between competitive sorption and concentration polarisation may be the reason for the levelling off in permeance beyond 20 mbar water partial pressure.

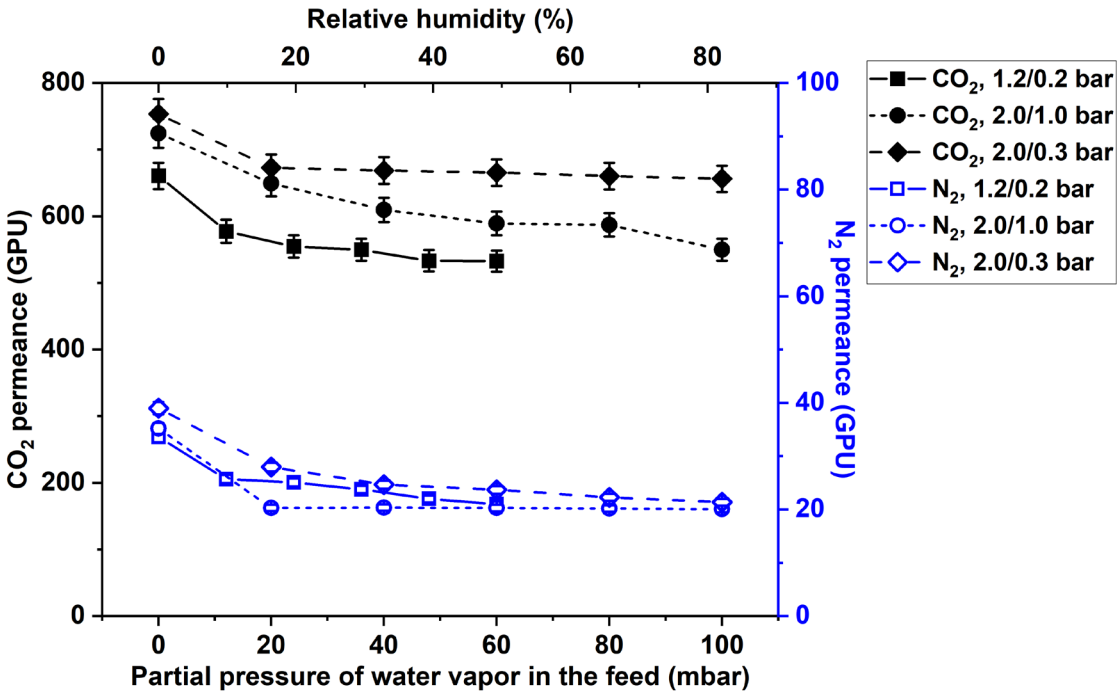

Figure 3. The influence of water vapor on the single gas permeance of CO_2 and N_2 at 50 ºC in different pressure conditions (closed symbol: CO_2, open symbol: N_2, square: 1.2/0.2 bar, circle: 2.0/1.0 bar and diamond: 2.0/0.3 bar)

Figure 4 shows the water permeance when supplied with CO_2 as the carrier gas. Water permeance did not change significantly with the feed pressure, or as the water vapor in the feed changed. Notably, the water permeance was 1090 ± 200 GPU, which is higher than that N_2 or CO_2. As a condensable gas, water has high solubility and its small size leads to high diffusivity[18, 35, 36]. Indeed, the value presented here may be lower than the true value, as concentration polarisation will lead to a slight reduction.

The comparable data for N_2 as a carrier gas is not shown. In this case, the data for water permeance fluctuated significantly with the feed gas pressure, probably as a result of increased concentration

polarisation. This phenomenon is exacerbated when there is a large difference between permeance values, as is the case for N_2 and H_2O. The permeate flowrates for these experiments was very low, and this made accurate measurement of the humidity difficult.

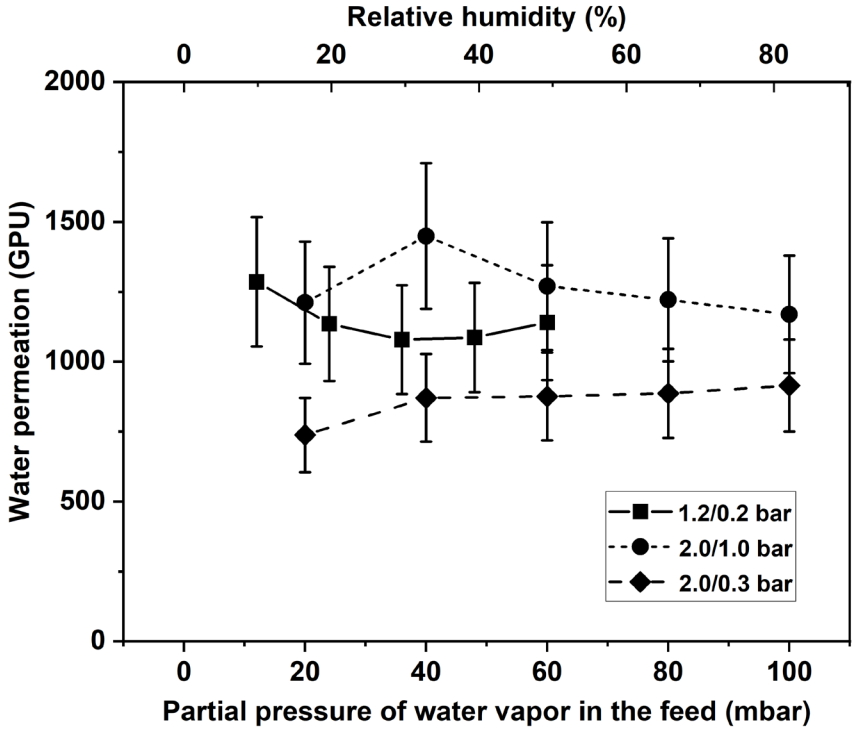

Figure 4: The water permeance at 50 ºC with CO_2 as the carrier gas under different pressure conditions (square: 1.2/0.2 bar, circle: 2.0/1.0 bar and diamond: 2.0/0.3 bar)

A CO_2/N_2 mixture gas was also tested in the presence of water vapor (Figure 5(a)). The gas composition was 14/86 (CO_2/N_2) at feed side and feed/permeate pressure was 2.0/0.2 bar, respectively. After the test under dry conditions, the water vapor in the feed stream was gradually increased to 100 mbar. The dry gas permeabilities were lower for both CO_2 and N_2 in the mixture than for the pure gases due to competitive sorption. The overall trends in gas permeability and CO_2/N_2 selectivity, however, were consistent with that observed for the pure gases. The CO_2

permeance fell from 430 to 390 GPU as the water content increased, while the N_2 gas permeance fell from 28 to 17 GPU. Mixed gas selectivity increased from 15 to 23 as the water content increased, similar to the trend observed for the pure gases. The concentration of CO_2 in the permeate (y_i) was enhanced from 60% to 67% as water vapor humidity increased, but there was a slight loss of recovery from 28% to 23% (Figure 5(b). The increase in CO_2 purity results from the increase in mixed gas selectivity, while the slight decrease of permeance causes the loss in recovery. This permeate concentration is comparable to that achieved in pilot scale trials of the Generation 1 Polaris membranes under commercialisation by MTR[37]. In the point of industrial application, a higher purity of CO_2 at the permeate side is required, but this is usually achieved through the use of a second membrane[38, 39] or cryogenic[40] stage. A longer module than that used in these laboratory scale experiments would allow for greater CO_2 recovery, albeit with a small loss in CO_2 purity[20]. The water permeance with this gas mixture was difficult to assess due to the concentration polarisation in this nitrogen-rich stream and so is not presented here.

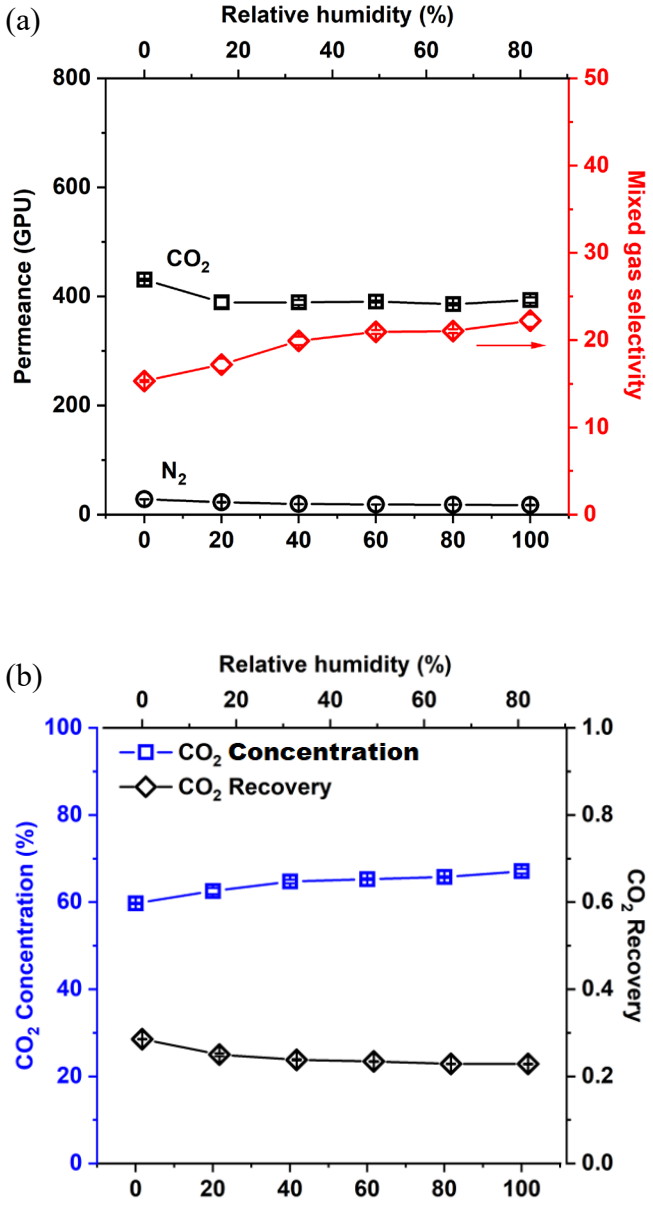

Figure 5. (a) The gas permeance and mixed gas selectivity of humidified mixed gas (feed pressure: 2.0 bar, permeate pressure: 0.2 bar, feed flow rate of gas mixture: 0.5 Nm^3/h, temperature: 50 °C), (b) CO_2 concentration and recovery on the permeate side of the system during the operation under these operating conditions.

3.2. Minor Component Testing

Figure 6 shows the gas permeances when a dry mixture of $CO_2/SO_2/O_2/N_2$ was tested over a period of 30 days. The membrane performance was very stable across the experimental periods and no plasticization or aging effects were observed, indicating its excellent performance, even with these toxic gases present. The permeances of SO_2, CO_2, O_2 and N_2 were 650 ± 50 GPU, 560 ± 20 GPU, 155 ± 5 GPU and 38 ± 2 GPU, respectively. The CO_2 permeance in the mixture was lower than that of the dry pure gas shown in Figure 3, which may be partly explained by the change in testing temperature from 50 °C to 30 °C, but higher than that for the gas mixture in Figure 5(a). The CO_2/N_2 selectivity was 15 ± 1, consistent with the mixed gas value shown in Figure 5(a).

SO_2 has a kinetic diameter of 3.6 Å, which is larger than that of CO_2 (3.3 Å). Hence, the higher permeance cannot be related to higher diffusivity. Conversely, it may be attributed to its higher condensability and thus solubility [15]. It is interesting that the SO_2/CO_2 selectivity was less than 1.2, while the literature data are in the range of 5-40 for bulk polymer (un-carbonised) films [15]. For instant, Lu et al. reported SO_2/CO_2 permselectivity of 3 for a dense cellulose triacetate (CTA) membrane at 35 °C [4]. This indicates that the current membrane shows less dependence upon solubility selectivity and is more dependent upon diffusivity selectivity for its performance.

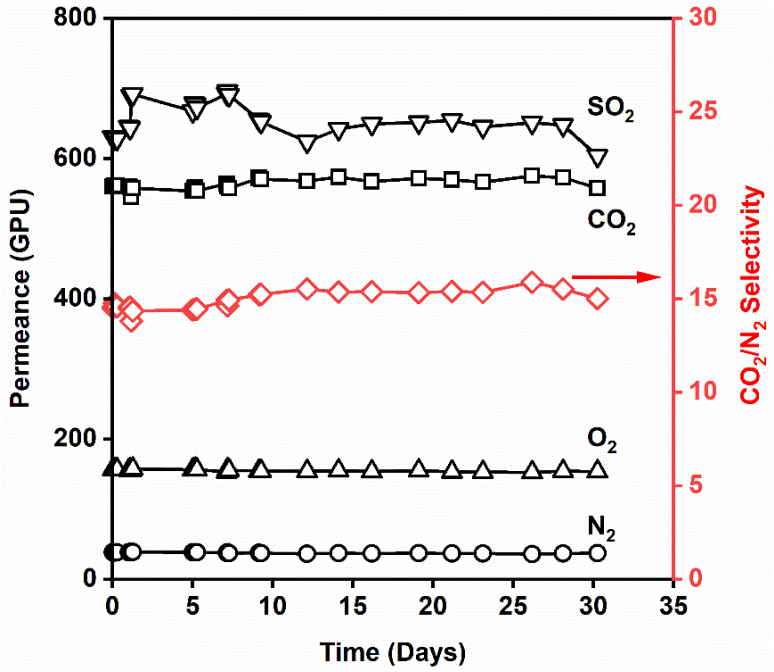

Figure 6. The influence of SO_2 on gas permeances and CO_2/N_2 selectivity as a function of time. The feed gas was $SO_2/CO_2/O_2/N_2$: 990 ppm/14.0%/6.04%/balance at a feed pressure of 2 bar and temperature of 30 °C.

For industrial mixed gas conditions, understanding the gas composition on the permeate side can be informative rather than the selectivity data. The permeate gas composition for the above test is shown in Figure 7. The membrane concentrates the SO_2, with this increasing from 990 ppm on the feed side to 4350 ± 150 ppm in the permeate side. This means that condensation of the water content downstream could lead to the formation of sulfuric acid, which is highly corrosive. Extra measures may be required to reduce the pH of any condensate even though SO_2 itself has no clear impact on the membrane performance. The CO_2 concentration was enriched from 14% on the feed side to 56% in the permeate side, while for N_2 it decreased from 80% to 35%. The CO_2 recovery is calculated as 51 ± 1%. As noted earlier, the use of a longer membrane module would enhance this recovery, while the use of a second stage would improve the CO_2 purity.

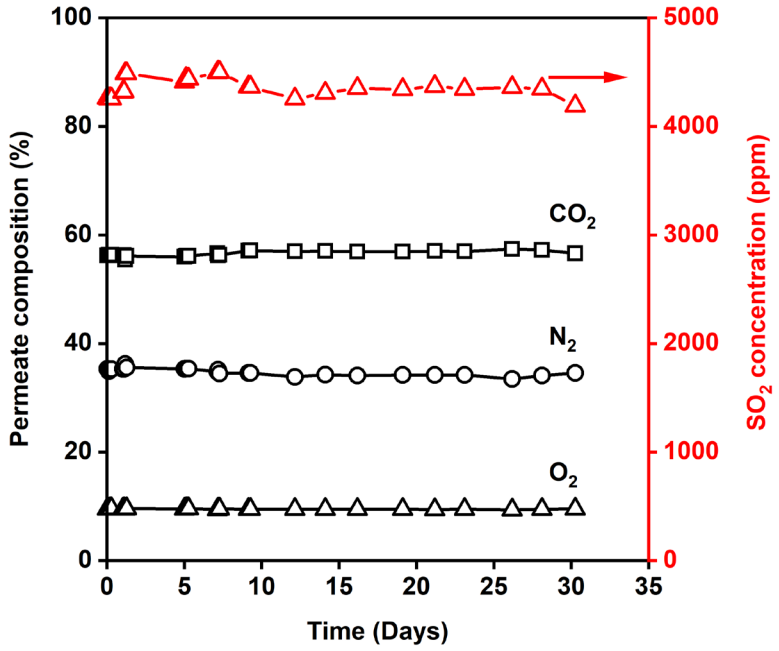

Figure 7. The influence of SO_2 on the gas composition on the permeate side as a function of time. The feed gas was $SO_2/CO_2/O_2/N_2$: 990 ppm/14.0%/6.04%/balance at a feed pressure of 2 bar and temperature of 30 °C.

The influence of NO on the membrane performance was also investigated for 30 days using another membrane module, and the results are shown in Figure 8. Similarly, the membrane maintained stable performance across the testing period. No clear plasticization was observed. The NO feed concentration in this case is higher than is commonly observed in post-combustion flue steams, which is 100-500 ppm [2, 41], so these results confirm that the membrane can withstand high NO concentrations, at least in a dry gas stream. The CO_2, NO and N_2 permeances were 500 ± 10 GPU, 125 ± 10 GPU and 29 ± 2 GPU, respectively. The CO_2/N_2 selectivity was 17 ± 2. The CO_2 and N_2 permeances are comparable with the membrane module for the SO_2 experiment shown in

Figure 6, indicating good reproducibility. Although NO has a smaller kinetic diameter (3.17 Å) than CO_2 (3.3 Å), it has a lower critical temperature (180 K) than CO_2 (304.2 K). As a result, the lower NO permeance suggests that the membrane separation is based on solubility rather than diffusivity. NO has higher permeance than N_2 as it has both a smaller kinetic dimeter and a higher critical temperature.

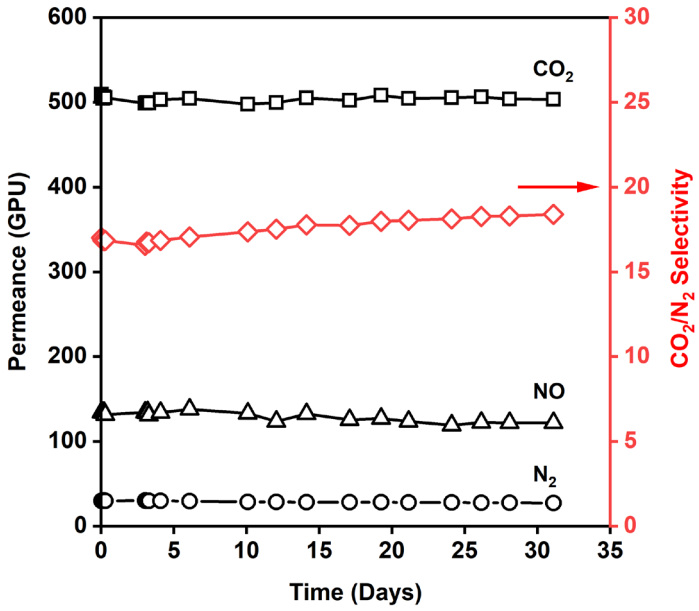

Figure 8. The influence of NO on gas permeance and CO_2/N_2 selectivity as a function of time. The feed gas was NO/CO_2/N_2: 990 ppm/13.4%/Balance at 2 bar pressure and temperature of 30 ^oC.

Similarly, the CO_2, N_2 and NO composition on the permeate side for this gas mixture are shown in Figure 9. NO was also enriched in the permeate stream, given its greater permeance relative to nitrogen. Again, this could result in issues with corrosion, should nitric acid form during the condensation of water in downstream equipment. The CO_2 concentration increased slightly across the experimental timeframe from 60.7 ± 0.1% to 62.6± 0.1% while the recovery was stable at 41± 0.4%.

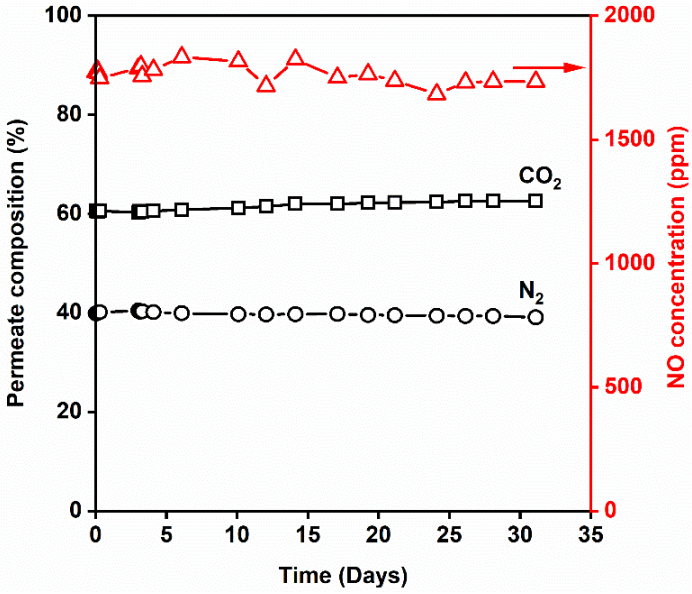

Figure 9. The influence of NO on the gas composition in the permeate side as a function of time. The feed gas was NO/CO_2/N_2: 990 ppm/13.4%/Balance at 2 bar pressure and temperature of 30 ^oC.

The above membrane module was further used to evaluate the influence of NO_2 on its performance and Figure 10 shows the permeances within a mixture of N_2, NO_2 and NO up to 50 hours. Their permeances were 27, 70 and 127 GPU, respectively. The N_2 and NO_2 permeances were identical to the data for the CO_2/NO/N_2 mixture shown in Figure 8, confirming the good accuracy of the experimental rig. The impact of NO_2 on the membrane performance was marginal in the experimental period. NO_2 has a similar critical temperature (431.4 K) as SO_2 [15], but the permeance was much lower than for this molecule. A similar trend has been reported for a thin zeolite ZSM-5 membrane [42]. This might partly be attributed to the fact that NO_2 is in equilibrium with the larger dimer, N_2O_4 which would diffuse more slowly. However, under the conditions tested here, the N_2O_4 content in the feed would only be 0.2% of the NO_2 content [43]. Pasternak et al.[27] determined a NO_2/CO_2 selectivity of around 13 in PTFE and attributed this high selectivity to the interaction

of NO_2 with the polar PTFE. Conversely, the calculated NO_2/CO_2 in the present case is much lower at around 0.25, indicating that the NO_2 solubility in this case is very low.

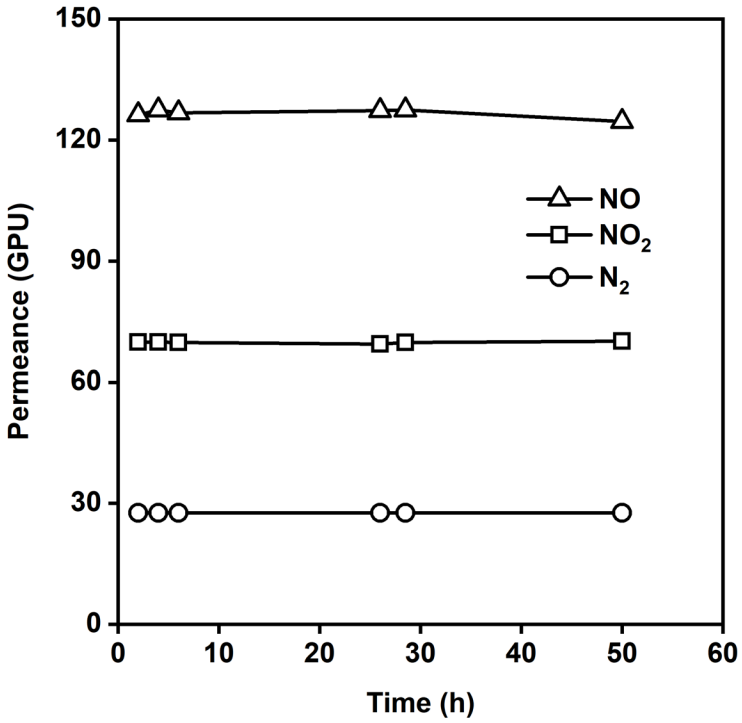

Figure 10. The influence of NO_2 on the membrane performance as a function of time. The feed gas was $NO_2/NO/N_2$: 205 ppm/750 ppm/balance at 2 bar pressure and temperature of 30 °C.

4. Conclusions

This work investigated the effect of common minor components including H_2O, SO_2, NO and NO_2 on the performance of a hollow fiber membrane module for post-combustion CO_2 capture. The CO_2 permeance was 660 GPU and the CO_2/N_2 permselectivity was 19 at 50 °C when 1 bar feed pressure was applied. CO_2 permeance slightly decreased whereas CO_2/N_2 selectivity increased when water vapor was present. At 49 RH% feed conditions, the CO_2 permeance was 530 GPU and the permselectivity increased to 25. The water vapor permeance was affected by the carrier gas on the feed side (i.e. CO_2 or N_2), due to the impact of concentration polarisation, which made accurate

measurement difficult. However, a value of 1090 ± 200 GPU was recorded when supplied with the more permeable CO_2. For the mixed gas test in the presence of water vapor, the gas permeance shows a reasonable range, 400 GPU and 30 GPU for CO_2 and N_2 permeance, respectively, with a resulting increase of mixed gas selectivity.

We also show that the water vapor did not severely influence CO_2 purity and recovery. The membrane was very stable for three different mixtures ($CO_2/SO_2/O_2/N_2$, $CO_2/NO/N_2$ and $NO/NO_2/N_2$) for up to 30 days. The permeances of SO_2, NO and NO_2 were 650, 125 and 70 GPU, respectively. The presence of SO_2, NO and NO_2 had marginal impact on the membrane performance.

Acknowledgements

This work was supported by the Korea Carbon Capture & Sequestration R&D Center (KCRC, NRF-2014M1A8A1049312) from the Ministry of Science, ICT and Future Planning.

Conflict of Interest Disclosure

The membrane module was provided by the Airrane Company.

Authorship

† J. H. Lee and Liang Liu contributed equally to this work.

References

1. Rogelj, J.; Meinshausen, M.; Knutti, R., Global warming under old and new scenarios using IPCC climate sensitivity range estimates. *Nature climate change* **2012,** 2, (4), 248-253.
2. Mumford, K. A.; Smith, K. H.; Anderson, C. J.; Shen, S.; Tao, W.; Suryaputradinata, Y. A.; Qader, A.; Hooper, B.; Innocenzi, R. A.; Kentish, S. E.;

Stevens, G. W., Post-combustion Capture of CO2: Results from the Solvent Absorption Capture Plant at Hazelwood Power Station Using Potassium Carbonate Solvent. *Energy & Fuels* **2012,** 26, (1), 138-146.
3. Samanta, A.; Zhao, A.; Shimizu, G. K.; Sarkar, P.; Gupta, R., Post-combustion CO2 capture using solid sorbents: a review. *Industrial & Engineering Chemistry Research* **2012,** 51, (4), 1438-1463.
4. Lu, H. T.; Kanehashi, S.; Scholes, C. A.; Kentish, S. E., The potential for use of cellulose triacetate membranes in post combustion capture. *International Journal of Greenhouse Gas Control* **2016,** 55, 97-104.
5. Merkel, T. C.; Lin, H.; Wei, X.; Baker, R., Power plant post-combustion carbon dioxide capture: An opportunity for membranes. *Journal of membrane science* **2010,** 359, (1-2), 126-139.
6. Qazi, S.; Gómez-Coma, L.; Albo, J.; Druon-Bocquet, S.; Irabien, A.; Sanchez-Marcano, J., CO2 capture in a hollow fiber membrane contactor coupled with ionic liquid: Influence of membrane wetting and process parameters. *Separation and Purification Technology* **2020,** 233, 115986.
7. Sohaib, Q.; Vadillo, J. M.; Gómez-Coma, L.; Albo, J.; Druon-Bocquet, S.; Irabien, A.; Sanchez-Marcano, J., Post-combustion CO2 capture by coupling [emim] cation based ionic liquids with a membrane contactor; Pseudo-steady-state approach. *International Journal of Greenhouse Gas Control* **2020,** 99, 103076.
8. Kim, S.; Scholes, C. A.; Heath, D. E.; Kentish, S. E., Gas-liquid membrane contactors for carbon dioxide separation: A review. *Chemical Engineering Journal* **2021,** 411.
9. Luis, P.; Van Gerven, T.; Van der Bruggen, B., Recent developments in membrane-based technologies for CO2 capture. *Progress in Energy and Combustion Science* **2012,** 38, (3), 419-448.
10. Robeson, L. M., Correlation of separation factor versus permeability for polymeric membranes. *Journal of membrane science* **1991,** 62, (2), 165-185.
11. Schmidt, P.; Lutze, P., Characterisation of organic solvent nanofiltration membranes in multi-component mixtures: Phenomena-based modelling and membrane modelling maps. *Journal of Membrane Science* **2013,** 445, (0), 183-199.
12. Koros, W. J.; Fleming, G., Membrane-based gas separation. *Journal of membrane science* **1993,** 83, (1), 1-80.
13. Brunetti, A.; Scura, F.; Barbieri, G.; Drioli, E., Membrane technologies for CO2 separation. *Journal of Membrane Science* **2010,** 359, (1-2), 115-125.
14. Alexander Stern, S., Polymers for gas separations: the next decade. *Journal of Membrane Science* **1994,** 94, (1), 1-65.
15. Scholes, C. A.; Kentish, S. E.; Stevens, G. W., Effects of Minor Components in Carbon Dioxide Capture Using Polymeric Gas Separation Membranes. *Separation & Purification Reviews* **2009,** 38, (1), 1-44.

16. Ansaloni, L.; Minelli, M.; Giacinti Baschetti, M.; Sarti, G. C., Effect of relative humidity and temperature on gas transport in Matrimid®: Experimental study and modeling. *Journal of Membrane Science* **2014,** 471, 392-401.
17. Scholes, C. A.; Freeman, B. D.; Kentish, S. E., Water vapor permeability and competitive sorption in thermally rearranged (TR) membranes. *Journal of Membrane Science* **2014,** 470, 132-137.
18. Chen, G. Q.; Kanehashi, S.; Doherty, C. M.; Hill, A. J.; Kentish, S. E., Water vapor permeation through cellulose acetate membranes and its impact upon membrane separation performance for natural gas purification. *Journal of Membrane Science* **2015,** 487, 249-255.
19. Anderson, C. J.; Tao, W.; Scholes, C. A.; Stevens, G. W.; Kentish, S. E. J. J. o. m. s., The performance of carbon membranes in the presence of condensable and non-condensable impurities. **2011,** 378, (1-2), 117-127.
20. Miandoab, E. S.; Kentish, S. E.; Scholes, C. A., Modelling competitive sorption and plasticization of glassy polymeric membranes used in biogas upgrading. *Journal of Membrane Science* **2021,** 617.
21. Thambimuthu, K.; Soltanieh, M.; Abandas, J. J. e. O. D., B. Metz, IPCC special report on carbon dioxide capture and storage. **2005,** 1, (6).
22. Kim, K.; Ingole, P. G.; Kim, J.; Lee, H., Separation performance of PEBAX/PEI hollow fiber composite membrane for SO2/CO2/N2 mixed gas. *Chemical Engineering Journal* **2013,** 233, 242-250.
23. Felder, R.; Spence, R.; Ferrell, J., Permeation of sulfur dioxide through polymers. *Journal of Chemical and Engineering Data* **1975,** 20, (3), 235-242.
24. Toy, L.; Kataria, A.; Gupta, R. *CO_2 Capture Membrane Process for Power Plant Flue Gas*; ; Research Triangle Institute International, Research Triangle Park, NC (United States): 2012; p Medium: ED; Size: 76 p.
25. Li, S.; Wang, Z.; He, W.; Zhang, C.; Wu, H.; Wang, J.; Wang, S., Effects of Minor SO2 on the Transport Properties of Fixed Carrier Membranes for CO2 Capture. *Industrial & Engineering Chemistry Research* **2014,** 53, (18), 7758-7767.
26. Scholes, C. A.; Chen, G. Q.; Stevens, G. W.; Kentish, S. E., Nitric oxide and carbon monoxide permeation through glassy polymeric membranes for carbon dioxide separation. *Chemical Engineering Research and Design* **2011,** 89, (9), 1730-1736.
27. Pasternak, R. A.; Christensen, M. V.; Heller, J., Diffusion and Permeation of Oxygen, Nitrogen, Carbon Dioxide, and Nitrogen Dioxide through Polytetrafluoroethylene. *Macromolecules* **1970,** 3, (3), 366-371.
28. Cui, L.; Qiu, W.; Paul, D. R.; Koros, W. J., Physical aging of 6FDA-based polyimide membranes monitored by gas permeability. *Polymer* **2011,** 52, (15), 3374-3380.

29. Kim, J.; Koros, W. J.; Paul, D. R., Effects of CO2 exposure and physical aging on the gas permeability of thin 6FDA-based polyimide membranes: Part 2. with crosslinking. *Journal of membrane science* **2006,** 282, (1-2), 32-43.
30. Hägg, M. B.; Lindbråthen, A.; He, X.; Nodeland, S. G.; Cantero, T., Pilot Demonstration-reporting on CO2 Capture from a Cement Plant Using Hollow Fiber Process. *Energy Procedia* **2017,** 114, 6150-6165.
31. Su Jung, J.; Joo Hwan, L.; Sang Hoon, H.; Hyung Chul, K.; Seong Yong, H., Study on the Gas Separation of Carbon Molecular Sieve (CMS) Membrane for Recovering the Perfluorocompound Gases from the Electronics Industry. *Membrane Journal* **2016,** 26, (3), 220-228.
32. Jung Moo, L.; Myeong Geon, L.; Se Jong, K.; Hyung Chul, K.; Sang Yong, N., Characterization of Gas Permeation Properties of Polyimide Copolymer Membranes. *Membrane Journal* **2015,** 25, (3), 223-230.
33. Lee, J. H.; Lee, J.; Jo, H. J.; Seong, J. G.; Kim, J. S.; Lee, W. H.; Moon, J.; Lee, D.; Oh, W. J.; Yeo, J.-g.; Lee, Y. M., Wet CO2/N2 permeation through a crosslinked thermally rearranged poly(benzoxazole-co-imide) (XTR-PBOI) hollow fiber membrane module for CO2 capture. *Journal of Membrane Science* **2017,** 539, (Supplement C), 412-420.
34. Chen, G. Q.; Scholes, C. A.; Qiao, G. G.; Kentish, S. E., Water vapor permeation in polyimide membranes. *Journal of Membrane Science* **2011,** 379, (1-2), 479-487.
35. Azher, H.; Scholes, C. A.; Stevens, G. W.; Kentish, S. E., Water permeation and sorption properties of Nafion 115 at elevated temperatures. *Journal of Membrane Science* **2014,** 459, 104-113.
36. Chen, G. Q.; Scholes, C. A.; Doherty, C. M.; Hill, A. J.; Qiao, G. G.; Kentish, S. E., Modeling of the sorption and transport properties of water vapor in polyimide membranes. *Journal of Membrane Science* **2012,** 409-410, 96-104.
37. White, L. S.; Amo, K. D.; Wu, T.; Merkel, T. C., Extended field trials of Polaris sweep modules for carbon capture. *Journal of Membrane Science* **2017,** 542, 217-225.
38. Giordano, L.; Roizard, D.; Bounaceur, R.; Favre, E., Evaluating the effects of CO2 capture benchmarks on efficiency and costs of membrane systems for post-combustion capture: A parametric simulation study. *International Journal of Greenhouse Gas Control* **2017,** 63, 449-461.
39. Merkel, T. C.; Lin, H.; Wei, X.; Baker, R., Power plant post-combustion carbon dioxide capture: An opportunity for membranes. *Journal of Membrane Science* **2010,** 359, (1), 126-139.
40. Belaissaoui, B.; Le Moullec, Y.; Willson, D.; Favre, E., Hybrid membrane cryogenic process for post-combustion CO2 capture. *Journal of Membrane Science* **2012,** 415-416, 424-434.

41. D'Alessandro, D. M.; Smit, B.; Long, J. R., Carbon dioxide capture: prospects for new materials. *Angewandte Chemie International Edition* **2010,** 49, (35), 6058-6082.
42. Perdana, I.; Creaser, D.; Lindmark, J.; Hedlund, J., Influence of NOx adsorbed species on component permeation through ZSM-5 membranes. *Journal of Membrane Science* **2010,** 349, (1-2), 83-89.
43. Roscoe, H. K.; Hind, A. K., The equilibrium constant of NO2 with N2O4 and the temperature dependence of the visible spectrum of NO2: A critical review and the implications for measurements of NO2 in the polar stratosphere. *Journal of Atmospheric Chemistry* **1993,** 16, (3), 257-276.